Time-Varying Effects in Models for Current-Mode Control

David J. Perreault George C. Verghese
Massachusetts Institute of Technology
Laboratory for Electromagnetic and Electronic Systems
Cambridge, MA 02139 USA

Abstract - **This paper investigates issues in modeling of current-mode control. The effects of the current-sampling intrinsic to current-mode control are analyzed, and inadequately recognized limitations of linear, time invariant models at high frequencies are exposed. The paper also examines the geometric methods used to derive duty ratio constraints in averaged models of current-mode control. The conclusions are supported by simulation and experimental results.**

I. Introduction

Modeling of current-mode controlled converters has been a topic of interest to the power electronics community for well over a decade. Recently, much effort has been focused on extending the traditional averaged models to capture high-frequency behavior [1-3]. Other research has been aimed at improving modeling accuracy by eliminating subtle flaws in the derivation of duty ratio constraints for current-mode control [4,5]. This paper investigates these recent modeling approaches, and in the process exposes some serious limitations that have not been adequately accounted for previously. Section II of the paper investigates the impact of sampled-data effects on small-signal modeling of current-mode controlled converters. Section III examines the geometric methods used to derive duty ratio constraints used for averaged models of current-mode control. Comparisons between models are made using the boost converter example from [2], shown in Fig. 1. Under normal operating conditions, the switch is turned on every T seconds, and is turned off when the inductor current $i_L(t)$ reaches a peak value of $i_p(t)$ minus a compensating ramp.

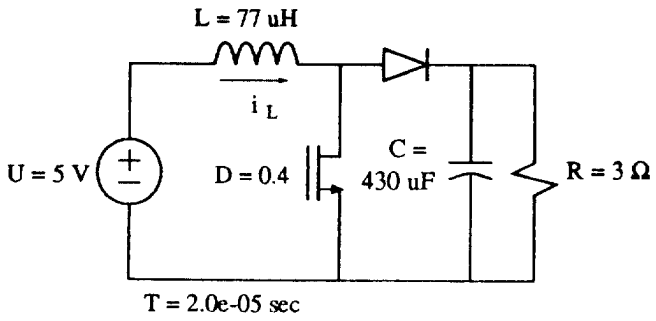

Figure 1 Example boost converter.

II. Sampled-Data Effects

Efforts to extend small-signal linear, time invariant (LTI) models of current-mode controlled converters to high frequencies have been motivated by the desire to improve control design while retaining simplicity. Typically, low-frequency averaged models are used for feedback control design, while a separate high-frequency model is used for slope compensation of the well-known ripple instability. This is done because low-frequency averaged models cannot predict the ripple instability, even under open-loop conditions. On the other hand, models used for predicting subharmonic oscillation do not always capture the behavior of converters operating under closed-loop voltage control. Thus, many researchers have sought to develop LTI transfer functions that fully capture the small-signal behavior of current-mode controlled converters [1-3,6]. Unfortunately, these works have not sufficiently addressed the limitations imposed by the current sampling intrinsic to current-mode control, leading to results that are subject to misinterpretation.

This section of the paper investigates the effects of current sampling, and assesses their impact on control design. As described in [1], and illustrated in Fig. 2, an approximate sample-and-hold relation exists between a perturbation $\hat{i}_p(t)$ in the control signal $i_p(t)$ and the resulting perturbation $\hat{i}_L(t)$ in

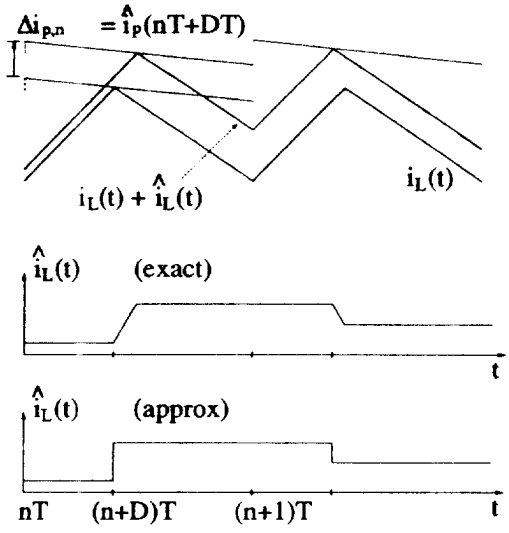

Figure 2 The approximate sample-and-hold relationship between perturbations in control and perturbations in (instantaneous and average) inductor current.

0-7803-2730-6/95 $4.00 © 1995 IEEE

inductor current $i_L(t)$ for an open-loop current-mode controlled converter. The corresponding perturbation in the one-cycle *average* inductor current $\hat{i}_L(t)$ is also $\hat{i}_L(t)$, to first order. These facts form the basis for the derivation in [1,2] of high-frequency extensions to low-frequency models. A similar approach, expressed in terms of duty ratio perturbations, is used in [3]. A more exact numerical approach to generating a transfer function is described in [6], but the limitations imposed by current sampling apply equally there as well. What is not made clear in all these works is that, because of the sampling and reconstruction, the system becomes significantly *time-varying* to perturbations in $i_p(t)$ that approach half the switching frequency. This leads to the injection of additional frequencies in $\hat{i}_L(t)$ and thereby causes significant deviations from the results suggested by existing treatments.

A. Modeling Approach

Consider the effect of a perturbation in the control signal $i_p(t)$ of a current-mode controlled converter. With the assumption that the input and output voltages do not vary significantly, the relation between the perturbation in control and the resulting current perturbation can be approximated by a sample-and-hold system, Fig. 2. That is, the exact current perturbation $\hat{i}_L(t)$ (which is the difference between the transient and steady-state currents) is well approximated by the Zero-Order Hold (ZOH) of its samples $\Delta i_{L,n}$ taken at the turn-off instants. As discussed in [1], the main effects not modeled by the sample-and-hold approximation are the variation in sampling time and the finite slope of the current perturbation transition. The samples $\Delta i_{L,n}$ of the instantaneous current perturbation can also be seen as approximate samples of the *average* current perturbation over the ensuing interval of length T. Discrete-time relations can now be formed between the samples $\Delta i_{p,n}$ of the control perturbation and samples $\Delta i_{L,n}$ of the average inductor current perturbation, as described in [1]. In the small-signal limit, the LTI model of [1,2] results, with z-transform transfer function given by

$$H(z) = \frac{\Delta i_L(z)}{\Delta i_p(z)} = \frac{(M_1 + M_2)z}{(M_c + M_1)z - (M_c - M_2)} \qquad (1)$$

where M_1, M_2, and M_c are the slope magnitudes of the rising inductor current, falling inductor current, and slope-compensation ramp, respectively, in the nominal steady-state. (To keep notation streamlined, we employ the same symbol for time-domain and transform-domain quantities, but using the arguments z and s to denote the z- and Laplace transforms, respectively.) Under the preceding assumptions, the relation between perturbations in control and perturbations in average inductor current can then be modeled as shown in Fig. 3. The impulse modulation represents the sampling action, while the Zero-Order Hold (ZOH) at the output reconstructs the continuous-time waveform. We use *C/D* to denote the conversion of an impulse train to a sequence of samples, and *D/C* to denote the inverse operation.

This model has been adopted in [1,2] since it predicts how an initial current perturbation will decay, and can predict open-loop subharmonic oscillations due to ripple instability, where a conventional averaged model cannot. The papers [1,2] then attempt to incorporate the sample-and-hold effect into continuous-time LTI models by finding a continuous-time transfer function for the system of Fig. 3. What is ignored in these works is that *the system in Fig. 3 is time-varying for control perturbations approaching half the switching frequency, and cannot be described by a transfer function at these frequencies*. That is, the response of the system in Fig. 3 (and the response of current-mode controlled converters) at these frequencies depends on the position of the control signal with respect to the sampling points. To see this, note that the sampling process, which is modeled by impulse modulation, generates replicas of the input frequency spectrum centered at multiples of the sampling (or switching) frequency, $f_{sw} = 1/T$:

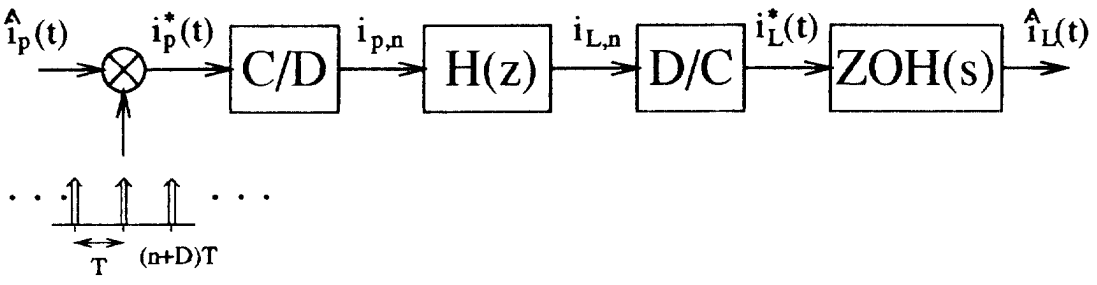

Figure 3 System for modeling the relation between perturbations in control and perturbations in current. This model relies on the assumptions used in forming $H(z)$.

$$\hat{i}_p^*(s) = \frac{1}{T}\sum_{n=-\infty}^{\infty} \hat{i}_p(s+\frac{2\pi nj}{T}) \ . \qquad (2)$$

The effects of the replicas are explicitly ignored in [1,2], which make the approximation:

$$\hat{i}_p^*(s) \approx \frac{1}{T}\hat{i}_p(s) \qquad (3)$$

to generate a control-to-current transfer function for the system of Fig. 3. For low-frequency perturbations, this approximation is justified, since the frequencies generated by the replicas will be well filtered by the low-pass ZOH reconstruction filter in Fig. 3. However, as can be inferred from the frequency response of the ZOH reconstructor, Fig. 4, the responses due to the replicas will not be well filtered for higher-frequency perturbations. This generates frequency components in the output that were not in the input, [7].

B. Simulation Results

To illustrate the preceding point, the converter of Fig. 1 was simulated for the nominal operating condition corresponding to $D = 0.4$ @ $I_p = 4.89$ A, $M_c = 0$, both with and without a small sinusoidal control perturbation at a given frequency. The difference between the inductor currents in the two cases is the small-signal response to the perturbation. As can be seen from the plots in Fig. 5, the response begins to deviate significantly from a sinusoid when the perturbation frequency is within a decade of the switching frequency. Furthermore, differently phased perturbations yield very different results. The frequency components due to the replicas are clearly visible in the output waveforms.

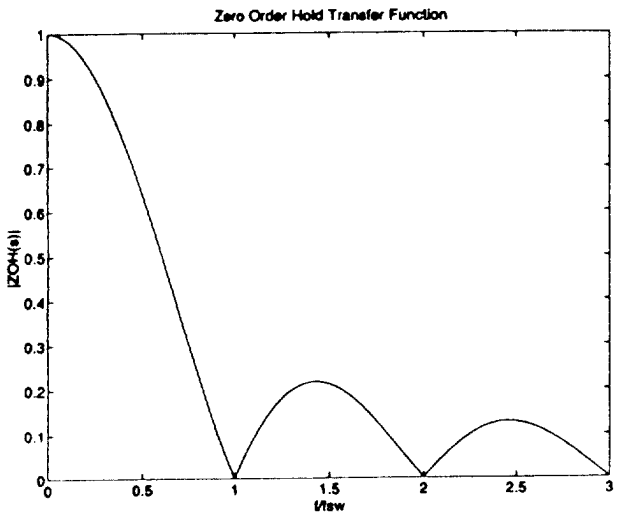

Figure 4 The frequency response of the Zero Order Hold reconstruction filter.

Similar effects occur in the output voltage waveforms.

What the works of [1-3,6] have set out to capture is the fundamental component of the response to a sinusoidal perturbation, in effect computing a describing function. This is why predictions in those works agree with narrow-band measurements made using network analyzers. However, models incorporating their approaches are not necessarily reliable for assessing closed-loop stability using LTI design methods. For example, consider the simulated response to a sinusoidal control perturbation at exactly half the switching frequency for the converter of Fig. 1 at the operating condition noted earlier. The amplitude of the perturbation is approximately 0.1% of the nominal $i_p(t) = I_p$, with the describing functions of [1,2] predicting a control-to-inductor-current gain of 3.2. However, because of the superposition of the input signal and one of its replicas at this frequency, the fundamental of the current response to this perturbation, Fig. 6, is approximately *twice as large* as predicted by the describing function of [1,2]. (The magnitude of the response plot is normalized to the perturbation magnitude.) The same magnification occurs in the voltage response. All of this suggests that there are significant dangers to making frequency response stability assessments using the LTI model. Furthermore, the displayed response is for a sine perturbation, with sampling occurring at points $nT+DT$, but differently phased perturbations will yield quite different results. Other interesting effects are also missed by the describing function approach. For example, a sinusoidal perturbation at $0.475f_{sw}$ yields output waveforms, Fig. 7, that exhibit strong beating due to the replica at $0.525f_{sw}$.

C. Experimental Results

To demonstrate these effects experimentally, the boost converter of Fig. 1 was constructed. The control circuit built allows one to set a nominal operating point I_p and separately inject an AC perturbation $i_p(t)$ on top of it. The perturbation signal is capacitively coupled to prevent DC operating point changes. Monitoring the inductor current with a wide-band spectrum analyzer allows all of the frequency components generated by a given perturbation to be observed. Figure 8 shows the spectrum of the response to small-signal perturbations at different frequencies. The observed responses closely match those predicted by our simulations and the time-varying model of Fig. 3. As half the switching frequency is approached, the replica harmonic components become significant. Clearly, an LTI model is insufficient for describing the system at these frequencies.

What may be concluded from these results is that adding complexity to low-frequency LTI models in an attempt to capture high-frequency behavior may be of limited value for control loop design. Of course, modeling the sampling and reconstruction process can add accuracy to LTI models at frequencies where time-varying effects are unimportant. For

example, as will be seen in Section III, the sampling effects are apparent in transfer function phase responses even below one-tenth the switching frequency. However, it must be stressed that, due to the time-varying nature of the system as half the switching frequency is approached, LTI model predictions are only reliable for frequencies well below half the switching frequency.

III. Evaluation Of Averaged Model Derivations

Large-signal, continuous-time averaged models for dc-dc converters are typically expressed in terms of the continuous duty ratio $d(t)$ used to control the converter. Here, $d(t)$ may be defined, [8], as the running average over the interval $[t-T,t]$ of the 0-1 switching function $q(t)$, see Fig. 9. In current-mode control, the duty ratio is implicitly determined by the circuit waveforms. As a result, an additional duty ratio constraint must be developed to model current-mode controlled converters. The duty ratio constraint relates the duty ratio to the control current and state variables of the converter, and its derivation is usually based on the geometry of the inductor current waveform. This section of the paper examines the geometric methods used to derive duty ratio constraints for averaged models of current-mode control.

Recently, it was pointed out that geometric derivations of the duty ratio constraint should be based on transient waveforms and not steady state waveforms, [4]. The correct process outlined in [4] can be understood in a general mathematical context. Consider the method for linearizing a continuous-time generalized state-space system, which comprises state equations along with algebraic constraints that determine some of the auxiliary variables occurring in the state equations. (This development closely follows the one for discrete-time systems presented in [8].) We start with the nonlinear, time-invariant generalized state-space system

$$\begin{aligned} \frac{dx}{dt} &= f(x(t),r(t),w(t)) \\ 0 &= g(x(t),r(t),w(t)) \end{aligned} \tag{4}$$

where x is the vector of state variables, r is the vector of inputs, and w is the vector of auxiliary variables. Given a constant nominal operating condition that satisfies

$$\begin{aligned} 0 &= f(X,R,W) \\ 0 &= g(X,R,W) \end{aligned} \tag{5}$$

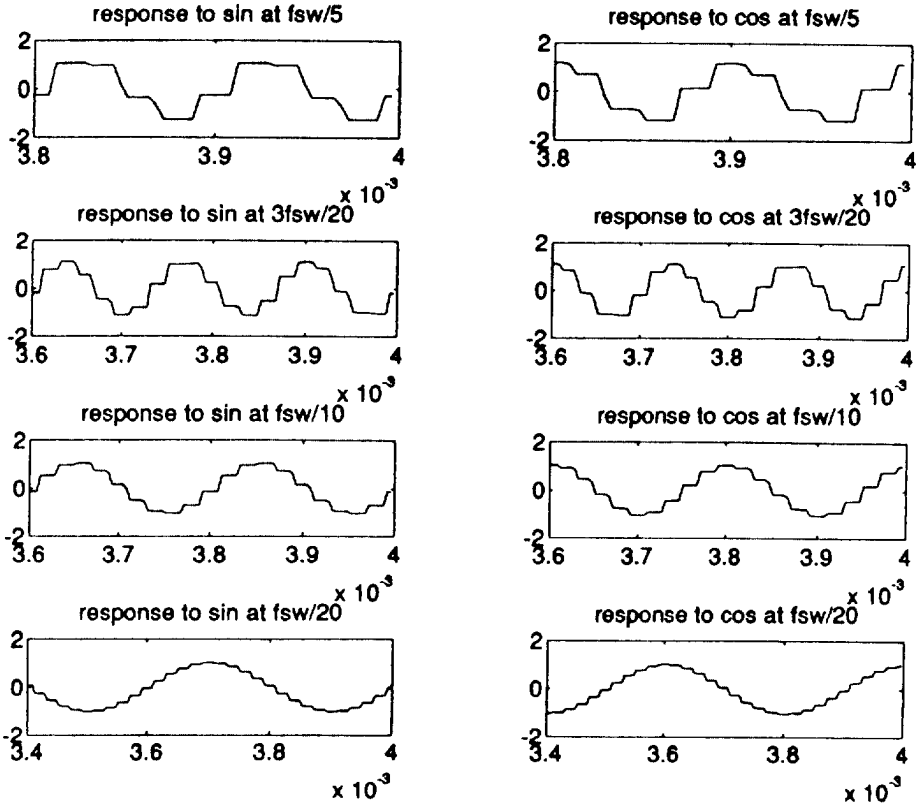

Figure 5 Small-signal inductor current response to sinusoidal control perturbations at various frequencies, for the converter of Fig. 1 ($I_p = 4.89, M_c = 0$). Response becomes nonsinusoidal above $f_{sw}/10$.

we consider deviations from this operating point such that

$$\begin{aligned} x(t) &= X + \hat{x}(t) \\ r(t) &= R + \hat{r}(t) \\ w(t) &= W + \hat{w}(t) \end{aligned} \quad . \tag{6}$$

If f, g are expanded in a multivariable Taylor series about the nominal operating condition, we find to first order that

$$\begin{aligned} \frac{d\hat{x}}{dt} &\approx \frac{\partial f}{\partial x}\hat{x} + \frac{\partial f}{\partial r}\hat{r} + \frac{\partial f}{\partial w}\hat{w} \\ 0 &\approx \frac{\partial g}{\partial x}\hat{x} + \frac{\partial g}{\partial r}\hat{r} + \frac{\partial g}{\partial w}\hat{w} \end{aligned} , \tag{7}$$

where all the partial derivatives denote *Jacobian matrices evaluated at the nominal operating point*. This is the linearized model and control constraint. Because the nonlinear model is time-invariant with a constant nominal solution, all the partial derivatives are constant, and the linearized model is therefore LTI. The second equation in (7) can be solved for $\hat{w}(t)$, and the result substituted in the first equation to get the desired linearized state-space model.

Now consider applying this linearization method to the state-space averaged model for current-mode control, which has the form of the first equation in (4), with $w(t) = d(t)$. We see that it is the large-signal (transient) duty ratio constraint that should be used as the second equation in (4) and differentiated. Only after differentiation should the Jacobians be evaluated at steady state.

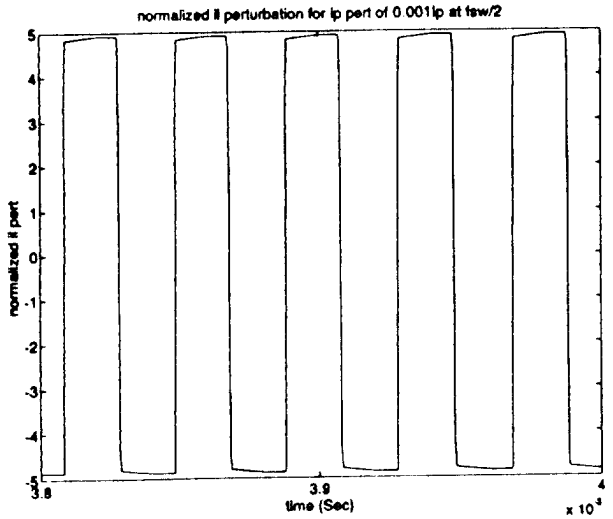

Figure 6 Small-signal inductor current response to a control perturbation of amplitude $0.001I_p$ at $f_{sw}/2$ in the boost converter of Fig. 1 ($D = 0.4$ @ $I_p = 4.89$ A, $M_c = 0$). The response is normalized to the amplitude of the perturbation.

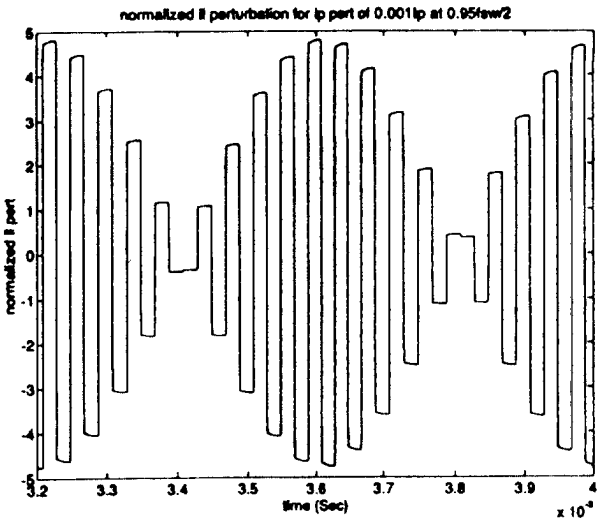

Figure 7 Small-signal inductor current response to a control perturbation of amplitude $0.001I_p$ at $0.95f_{sw}/2$ in the boost converter of Fig. 1 ($D = 0.4$ @ $I_p = 4.89$ A, $M_c = 0$). The response is normalized to the amplitude of the perturbation.

Consider the geometric evaluation of the duty ratio constraint, which describes the (local, running) average inductor current $\bar{i}_L(t)$ as a function of the continuous duty ratio $d(t)$ and control $i_p(t)$. The large-signal duty ratio constraint is usually evaluated at the end of the n^{th} cycle, where the duty ratio d_n equals $d(t)$, yielding

$$\bar{i}_L = i_p - M_c dT - \tfrac{1}{2}m_1 d^2 T - \tfrac{1}{2}m_2 d'^2 T \tag{8}$$

where $d' = 1-d$. Now linearize this expression as described above, and substitute in the proper waveform slopes for the boost converter, namely

$$\hat{m}_1 = \frac{\hat{u}}{L}, \quad \hat{m}_2 = \frac{\hat{v} - \hat{u}}{L} \tag{9}$$

where $u(t)$ and $v(t)$ are the input and output voltages, respectively. This yields the corrected control constraint of [4], see Table 1 here.

However, many small-signal models [1-3,9,10] explicitly or implicitly evaluate the large-signal duty ratio constraint at steady state *before* the linearization process. Furthermore, depending on how the incorrect steady-state constraint is applied, they arrive at different small-signal duty ratio constraints, Table 1. In the conventional method [9], the steady-state constraint $m_1 d = m_2 d'$ is applied to (8) before linearizing, yielding

$$\hat{i}_L = i_p - M_c dT - \tfrac{1}{2}m_1 dT \; . \tag{10}$$

Directly linearizing (10) and substituting in the relations (9) yields the conventional constraint of [9,10]. However, if we apply the steady-state constraint again, as is done in [2], we find for the boost converter that

$$m_1 = \frac{u}{L} = d'v. \qquad (11)$$

Substituting this relation into (10) and linearizing yields the different duty ratio constraint of [2]. The papers [1,3] use steady-state assumptions in yet another manner, implicitly assuming in their constraint computation that, regardless of the perturbation in duty cycle due to the rising part of the waveform, the inductor current returns to its previous minimum value by the end of the cycle. This yields yet another duty ratio constraint. These inconsistencies illustrate the problems associated with treating steady-state relationships as dynamic.

As it turns out, all of these constraints lead to essentially the same small-signal LTI model predictions at low frequencies. We offer the following explanation. The duty ratio constraint that leads to the expression used in [4] is derived over a certain window of length T. If the computations are instead carried out over displaced versions of this window, the resulting constraints vary from that given at the top of Table 1 by a term proportional to $m_1 d - m_2 d'$. Hence, the constraint used in [4] is well behaved only for operating conditions in which all of the constraints in Table 1 yield similar results.

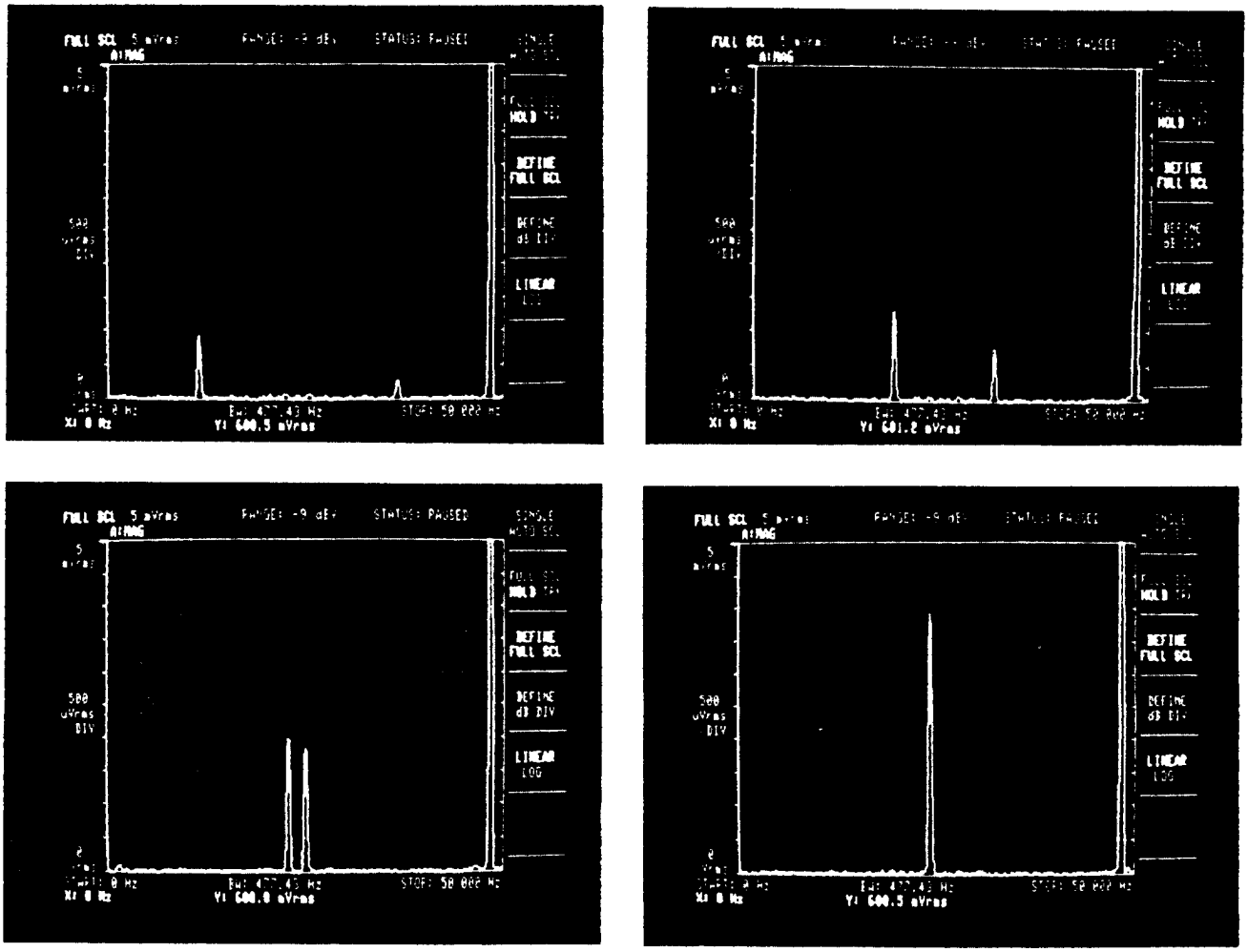

Figure 8 Inductor current spectra for sinusoidal control perturbations ($f_m \approx 48$ kHz). (A) 12 kHz (B) 18 kHz (C) 23 kHz (D) 24 kHz, constructive phase.

$\hat{d} = \frac{1}{M_c T}(\hat{i}_p - \hat{i}_L) - \frac{D^2}{2L}\hat{u} - \frac{D^{/\!/}}{2L}\hat{v}$	[4]
$\hat{d} = \frac{1}{(M_c + \frac{U}{2L})T}[\hat{i}_p - \hat{i}_L - \frac{DT}{2L}\hat{u}]$	[9,10]
$\hat{d} = \frac{2L}{(D' + \frac{2M_c L D'}{U} - D)VT}[\hat{i}_p - \hat{i}_L - \frac{DD'T}{2L}\hat{v}]$	[2]
$\hat{d} = \frac{1}{(\frac{U}{L} + M_c)T} \cdot [\hat{i}_p - \hat{i}_L - \frac{DT}{L}(1 - \frac{D}{2} + \frac{D^{/\!/}}{2D})\hat{u} + \frac{D^{/\!/}T}{2L}\hat{v}]$	[1,3]

Table I Duty ratio constraints used in various current-mode control models for the boost converter.

To see that the low-frequency performance characteristics of the conventional model [9,10] and the models of [1-3] are similar to models based on the corrected approach, consider the plots of Figs. 10 and 11, which show the small-signal control-to-current and control-to-output frequency responses for the various models. To separate the issue of correct duty-ratio constraints from the issue of high-frequency modeling addressed in Section II, the additional high frequency extensions proposed in [1-3] have not been incorporated. Samples of the frequency responses determined by simulating the system with and without a perturbation and looking at the difference in response are also plotted. As can be seen, all of these models yield similar results in the magnitude response up to a decade below the switching frequency. There are some differences in the phase responses even below a tenth the switching frequency.

It is certainly legitimate to ask how an LTI model may be refined to improve its prediction of the phase characteristic at these *low* frequencies, where the time-varying effects noted in Section II are *not* significant. For instance, including a phase delay of $\omega T/2$ with the model from [4], in order to capture the effect of the Zero Order Hold in Fig. 3, will lead to phase characteristics more closely matching those computed via simulation (indicated by the crosses in Figs. 10,11). Similarly, the high-frequency extensions proposed in [1-3], which are again aimed at capturing the effects of sampling and reconstruction, will have beneficial effects on capturing the phase characteristic at lower frequencies.

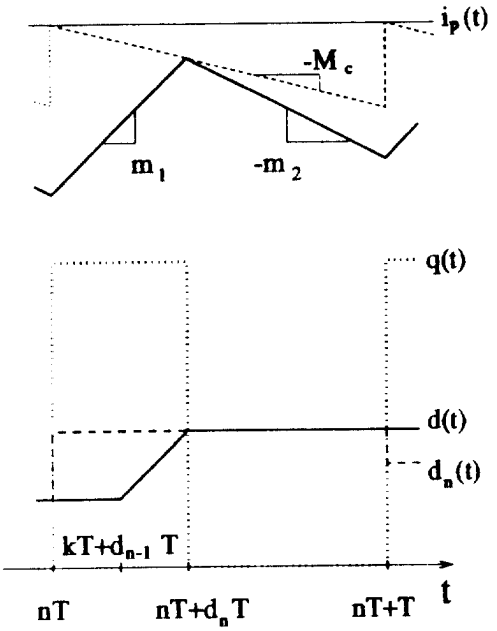

Figure 9 Inductor current waveforms for constant-frequency current-mode control, with relationships between $q(t)$, $d(t)$, d_n, $i_L(t)$, and $i_p(t)$.

IV. Conclusion

This paper has looked at several aspects of modeling current-mode controlled converters. It has been shown that current-mode controlled converters become significantly time-varying as half the switching frequency is approached. It is concluded that averaged LTI control models are only reliable for frequencies well below half the switching frequency, and are not suitable for predicting subharmonic oscillations due to ripple instabilities.

The geometric methods used to derive duty ratio constraints have also been examined. It has been confirmed that from a mathematical point of view, duty ratio constraints should be based on transient waveforms. It is also shown that *both* the conventional and corrected approaches are limited in accuracy when the system deviates significantly from steady state. This leads to similar performance of these models for frequencies at which they can be considered useful. Issues similar to those exposed here for current-mode control may be expected to arise in other contexts where refinement of averaged models is sought.

Acknowledgments

The authors would like to thank Professors Martin Schlecht and Steven Leeb of M.I.T. for their advice and comments during the course of this research. Generous equipment grants from the Intel and Tektronix Corporations facilitated the research and are greatly appreciated. David Perreault

gratefully acknowledges support from both the Bose Foundation and an IEEE Convergence Fellowship in Transportation Electronics.

REFERENCES

[1] R. Ridley, "A New, Continuous-Time Model for Current-Mode Control", *IEEE Transactions on Power Electronics*, Vol. 6, No. 2, April 1991, pp. 271-280.

[2] F. Tan and R. Middlebrook, "Unified Modeling and Measurement of Current-Programmed Converters", *IEEE Power Electronic Specialists Conference*, 1993, pp. 380-387.

[3] R. Tymerski and D. Li, "State Space Models for Current Programmed Pulse Width Modulated Converters", *IEEE Power Electronic Specialists Conference*, 1992, pp. 337-344.

[4] G. Verghese, C. Bruzos, and K. Mahabir, "Averaged and Sampled-Data Models for Current Mode Control: A Reexamination", *IEEE Power Electronics Specialists Conference*", 1989, pp.484-491.

[5] F. Rodriguez and J. Chen, "A Refined Nonlinear Averaged Model for Constant Frequency Current Mode Controlled PWM Converters", *IEEE Transactions on Power Electronics*, Vol. 6, No. 4, October 1991, pp. 656-664.

[6] R. Tymerski, "Application of the Time-Varying Transfer Function for Exact Small-Signal Analysis", *IEEE Power Electronics Specialists Conference*, 1991, pp. 80-87.

[7] G. Franklin, J. Powell, and M. Workman, Digital Control of Dynamic Systems, Second Ed., Addison Wesley, 1990, pp. 101-130.

[8] J. Kassakian, M. Schlecht, and G. Verghese, Principles of Power Electronics, Addison Wesley, 1991.

[9] S. Hsu, A. Brown, L. Rensink, and R. Middlebrook, "Modelling and Analysis of Switching DC-to-DC Converters in Constant-Frequency Current-Programmed Mode", *IEEE Power Electronics Specialists Conference*, 1979, pp. 284-301.

[10] R. Middlebrook, "Topics in Multiple-Loop Regulators and Current-Mode Programming", *IEEE Power Electronics Specialists Conference*, 1985, pp. 716-732.

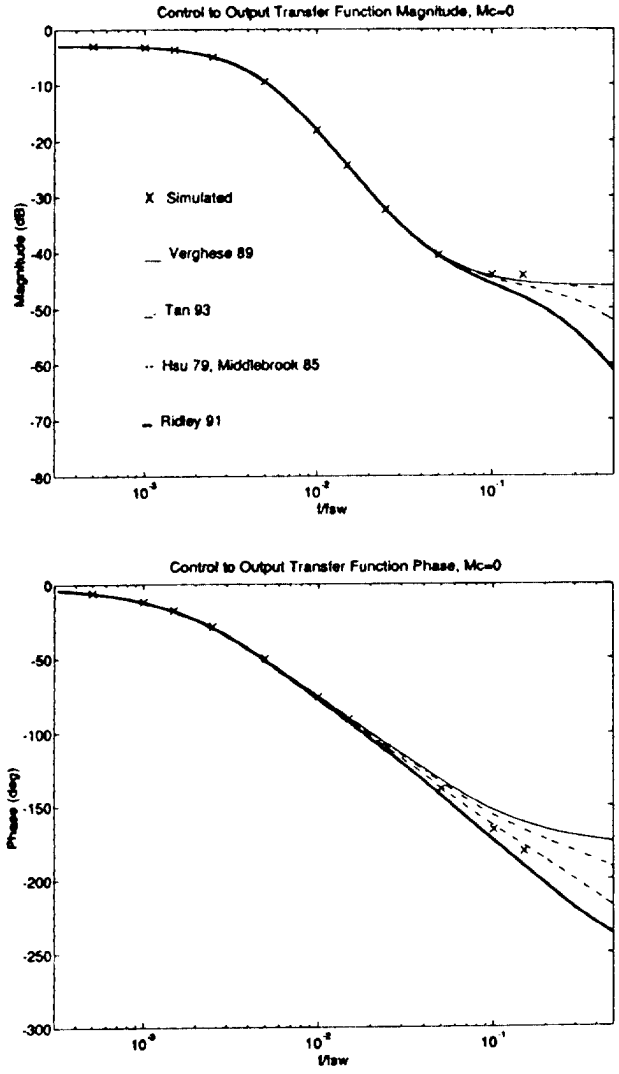

Figure 10 Small-signal control-to-output frequency responses of various averaged models for the boost converter of Fig. 1 (D = 0.4 @ I_p = 4.89, M_c =0).

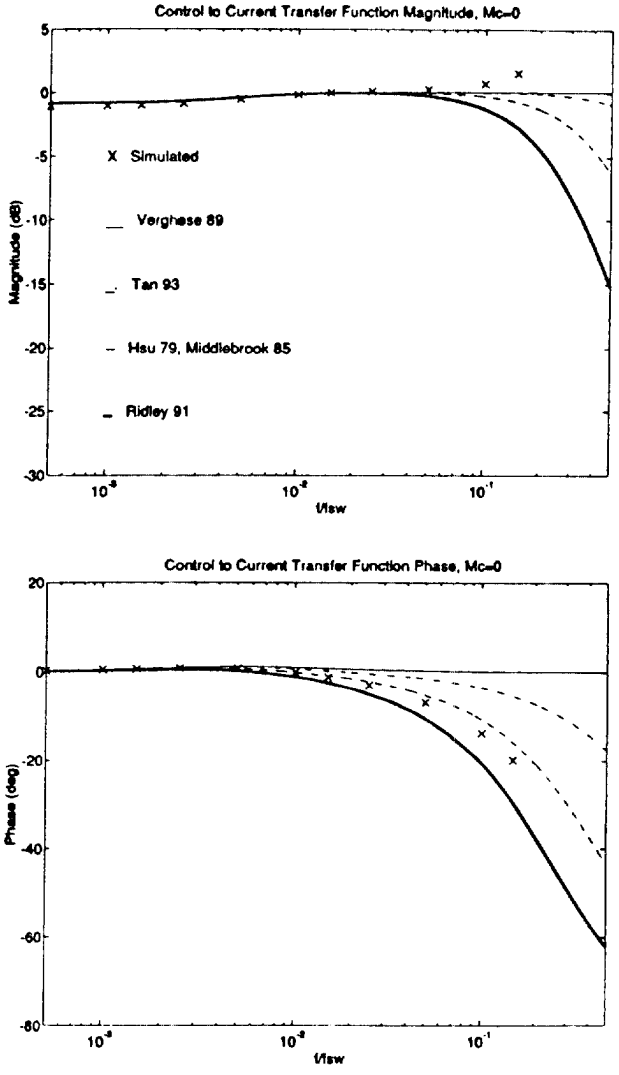

Figure 11 Small-signal control-to-inductor current frequency responses of various averaged models for the boost converter of Fig. 1 (D = 0.4 @ I_p = 4.89, M_c =0).